International Journal of Power Electronics and Drive System (IJPEDS)
Vol. 17, No. 3, September 2026, pp. 1962~1973
ISSN: 2088-8694, DOI: 10.11591/ijpeds.v17.i3.pp1962-1973

Comparation analysis of SSA and GWO algorithms for maximum power point tracking in standalone solar modules

Indhana Sudiharto, Mochammad Machmud Rifadil, Muhammad Affid Febriansyah
Industrial Electrical Engineering, Electronic Engineering Polytechnic Institute of Surabaya, Surabaya, Indonesia

Article Info

Article history:

Received Aug 13, 2025
Revised May 18, 2026
Accepted Jul 8, 2026

Keywords:

Convergence performance
MPPT optimization
Photovoltaic systems
Salp swarm algorithm
Sepic converter

ABSTRACT

Solar photovoltaic (PV) systems experience continuous output fluctuations due to changes in solar irradiance and operating temperature, reducing the effectiveness of power extraction. To improve energy harvesting capability, an adaptive maximum power point tracking (MPPT) method is required. This study evaluates the performance of the salp swarm algorithm (SSA) and grey wolf optimization (GWO) for MPPT control in a 100 Wp standalone PV system employing a single-ended primary inductor converter (SEPIC). The analysis focuses on tracking speed, efficiency, and stability under varying environmental conditions. Simulations were carried out in the ALTAIR PSIM Professional 2022.1.0.8 platform with irradiance levels ranging from 200–1000 W/m² and temperatures between 35-55 °C, including dynamic irradiance transitions. The obtained results show that SSA achieved a higher average tracking efficiency of 97.46% with a convergence time of 0.2276 s, while GWO produced 87.94% efficiency and a 0.2512 s convergence time. In addition, SSA demonstrated more stable tracking behavior and lower oscillation during low-irradiance operation. These results indicate that SSA provides better MPPT performance for compact standalone PV applications operating under fluctuating environmental conditions. Future work will involve hardware-based validation and real-time implementation.

Corresponding Author:

Mochammad Machmud Rifadil
Department of Electrical Engineering, Industrial Electrical Engineering
Electronic Engineering Polytechnic Institute of Surabaya
PENS Campus, Sukolilo, Surabaya 60111, Indonesia
Email: mmrifadil@pens.ac.id, mmrifadil@gmail.com

1. INTRODUCTION

The increasing demand for sustainable electrical energy has accelerated the development of renewable energy technologies, particularly solar photovoltaic (PV) systems, as an alternative to conventional fossil-based generation [1], [2]. PV technology has been broadly adopted in residential, industrial, educational, and public infrastructure applications because of its ability to directly convert solar radiation into electrical energy without producing environmental pollution [3]. In addition, PV systems offer several operational advantages, including simple installation, low maintenance requirements, and reduced operational costs [4]. Nevertheless, the electrical characteristics of PV modules are strongly influenced by environmental parameters, especially solar irradiance and operating temperature, resulting in continuous variations in output voltage, current, and generated power [5], [6].

To maximize energy extraction, PV systems require maximum power point tracking (MPPT) controllers capable of maintaining operation at the optimal power point under changing atmospheric conditions. Conventional MPPT techniques such as perturb and observe (P&O), incremental conductance

(INC), and fuzzy logic control (FLC) remain widely utilized because of their relatively simple implementation and low computational complexity [7]-[9]. However, these approaches frequently experience oscillatory behavior around the maximum power point and reduced tracking precision during rapid irradiance transitions, leading to power losses and slower dynamic response [10], [11].

In recent years, optimization-based MPPT strategies inspired by natural intelligence have received considerable attention to overcome the limitations of classical methods. Algorithms such as particle swarm optimization (PSO), genetic algorithm (GA), grey wolf optimization (GWO), and salp swarm algorithm (SSA) have demonstrated promising capability in nonlinear optimization problems associated with PV energy conversion systems [12]-[15]. Among these methods, SSA exhibits strong exploration and exploitation characteristics that enable rapid convergence while minimizing the risk of trapping in local optima [16]. The optimization mechanism of SSA is derived from the chain movement behavior of salp populations in marine environments and has been successfully implemented in several engineering optimization applications, including renewable energy systems [16], [17]. Previous investigations reported that SSA can provide improved tracking accuracy and enhanced transient response compared to several conventional and metaheuristic MPPT approaches under varying irradiance conditions [18]-[20].

Although numerous MPPT studies have been conducted for PV systems, most investigations primarily focus on large-scale PV arrays operating under partial shading conditions, where multiple local maxima frequently occur due to nonuniform irradiance distribution. Comparatively fewer studies discuss the performance of advanced optimization algorithms in standalone single-panel PV configurations operating under uniformly distributed but dynamically fluctuating environmental conditions. In practical implementation, single-panel PV systems remain highly vulnerable to rapid irradiance disturbances caused by cloud movement, dust accumulation, and temperature variation, which continuously shift the maximum power point location [6], [21]. These conditions are particularly relevant in compact PV applications such as portable power units, street lighting systems, remote monitoring devices, and internet of things (IoT)-based energy systems, where fast tracking capability and stable power extraction are critically required [22].

Furthermore, previous studies generally emphasize hybrid MPPT structures or comparisons involving conventional techniques, while comprehensive analysis specifically comparing SSA and GWO performance in single-module PV systems remains limited. Existing literature rarely discusses the dynamic behavior, convergence characteristics, and low-irradiance stability of these algorithms within simplified standalone PV architectures. Consequently, a research gap still exists regarding the effectiveness of SSA relative to GWO for maintaining stable and accurate MPPT performance under rapidly changing operating conditions.

Therefore, this study presents a comparative evaluation of SSA and GWO for MPPT implementation in a 100 Wp standalone PV system employing a single-ended primary inductor converter (SEPIC). The investigation focuses on tracking efficiency, convergence speed, transient response, and output stability under varying irradiance and temperature conditions. By concentrating on a compact single-panel configuration, this work provides a clearer assessment of algorithm behavior under dynamic environmental changes and contributes to the development of reliable MPPT strategies for small-scale real-time PV applications.

2. METHOD

This study develops an MPPT system based on the SSA for a standalone PV module operating under dynamically changing environmental conditions. The proposed configuration consists of a 100 Wp PV module, voltage and current sensing units, a SEPIC, a battery storage unit, and an STM32-based control system responsible for executing the MPPT algorithm and regulating the converter duty cycle. The complete configuration of the proposed system is illustrated in Figure 1. The sensing stage continuously measures PV voltage and current signals, which are processed by the controller to determine the optimal duty cycle corresponding to the maximum power point.

The PV system was evaluated under irradiance variations ranging from 200–1000 W/m² and temperature conditions between 35–55 °C to investigate transient behavior, tracking stability, and convergence performance during environmental fluctuations. In addition, rapid irradiance transition scenarios were introduced to emulate realistic atmospheric disturbances such as cloud movement and temporary shading effects. This approach enables the evaluation of algorithm robustness under continuously changing operating conditions. Compared with conventional MPPT techniques such as P&O and INC, optimization-based algorithms provide better adaptability for nonlinear PV characteristics and rapidly changing irradiance profiles [23], [24]. Among various optimization approaches, SSA was selected because of its strong global searching capability, balanced exploration–exploitation mechanism, and stable convergence behavior. These characteristics enable the algorithm to minimize oscillation around the maximum power point while maintaining fast response performance. To provide a fair comparative evaluation, GWO was implemented using identical operating conditions, converter parameters, and simulation scenarios.

2.1. Maximum power point tracking

MPPT is implemented to maintain the PV module operation at the optimal voltage and current point where the generated power reaches its maximum value. Due to continuous variations in irradiance and temperature, the maximum power point position changes dynamically over time. Therefore, the controller continuously updates the converter duty cycle to maintain optimal operating conditions and reduce power loss.

As shown in Figure 2, the MPPT mechanism regulates the operating voltage relative to the maximum power point voltage (Vmp). When the operating voltage falls below Vmp, the controller increases the converter duty cycle to raise the operating voltage. Conversely, when the operating voltage exceeds Vmp, the duty cycle is reduced until the operating point converges toward the peak power region [25]. This iterative process allows the system to sustain maximum energy extraction under fluctuating environmental conditions.

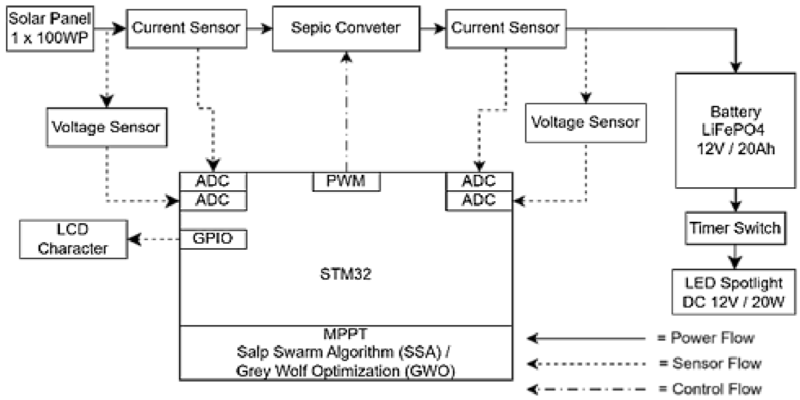

Figure 1. System diagram block

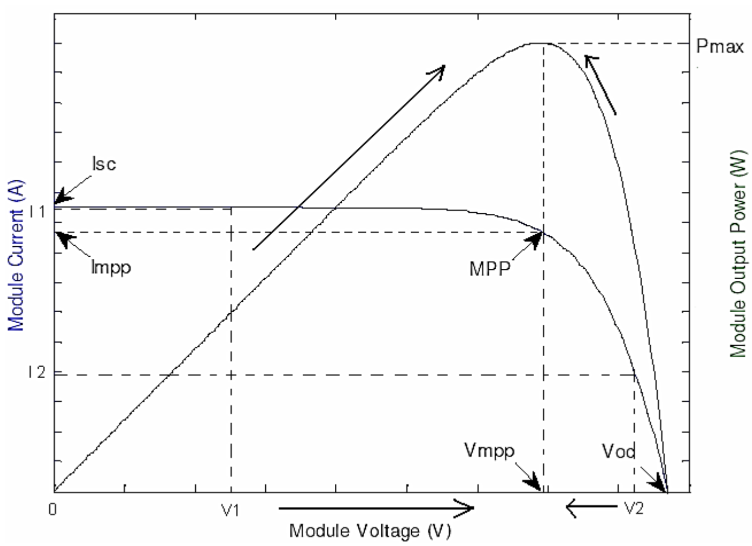

Figure 2. MPPT voltage rise and fall curve [25]

2.2. Salp swarm algorithm (SSA)

The SSA is a swarm intelligence optimization technique inspired by the chain movement behavior of salps in marine environments. The population structure consists of a leader and multiple followers, where the leader directs the searching process while follower positions are updated based on the movement of preceding salps. In the MPPT application, each salp represents a candidate duty cycle value for the SEPIC converter.

The leader position update mechanism is expressed as (1):

$$X_j^1 = \begin{cases} F_j + c_1((ub_j - ib_j)c_2 + ib_j) & C_3 \geq 0.5 \\ F_j - c_1((ub_j - ib_j)c_2 + ib_j) & C_3 < 0.5 \end{cases} \quad (1)$$

Where F_j denotes the food source position in the j^{th} dimension, ub_j and lb_j represents the upper and lower bounds of the search space, and c_1, c_2, and c_3 are random coefficients. The parameter c_1 controls the balance between exploration and exploitation and is defined as (2).

$$C_1 = 2e^{-\left(\frac{4l}{L}\right)^2} \quad (2)$$

Where L represents the maximum number of iterations, and I is the current iteration. The coefficients c_2 and c_3 are uniformly distributed random numbers in the interval [0, 1], controlling the direction and step size of the search. The follower positions are updated based on Newton's law of motion:

$$x_J^1 = \frac{1}{2}at^2 + v_0 t \quad (3)$$

Where $i \geq 2$, x_J^1 represents the position of the i^{th} follower in the j dimension, t denotes time, v_0 is the initial velocity, and $a = \frac{v_{\text{final}}}{v_0}$ is defined where we have $v = \frac{x - x_0}{t}$.

The (3) can be reduced as follows, taking into account $v_0 = 0$, since there is a one-time difference between iterations and time is constant across them.

$$x_J^1 = \frac{1}{2}at^2 + v_0 t \quad (4)$$

Where $i \geq 2$, and x_J^1 denotes the position of the i^{th} follower Salp in the j^{th} dimension [17]. This mechanism enables smooth convergence while preventing sudden oscillatory movement during the searching process.

To ensure reproducibility and parameter consistency, the SSA configuration used in this study was fixed throughout all simulation scenarios. The algorithm employed 30 salps with a maximum iteration limit of 100. The search space was constrained within the converter duty cycle range between 0 and 1 using uniformly distributed initialization. The fitness function was defined as the instantaneous PV output power, where the algorithm continuously searched for the duty cycle corresponding to the maximum power point. Sampling time was synchronized with the simulation step size to maintain numerical stability and fast transient response. In addition to steady-state evaluation, sensitivity analysis was conducted by observing the effect of iteration number and population size on tracking response and convergence behavior. This analysis was performed to examine algorithm robustness and computational consistency under dynamic operating conditions.

2.3. SSA parameter configuration

To ensure reproducibility and a fair performance evaluation, the configuration parameters of the SSA are explicitly defined in this study. The SSA is implemented to optimize the duty cycle of the SEPIC converter within a bounded search space corresponding to the allowable duty cycle range.

The key parameters used in the SSA implementation are summarized as follows:

i) Population size (N): 30 salps
ii) Maximum number of iterations (L): 100
iii) Search space boundaries: Duty cycle range limited between 0 and 1
iv) Initialization method: Uniform random distribution within the search bounds
v) Leader–follower structure: First salp acts as leader, remaining as followers
vi) Coefficient parameters c_1, c_2, and c_3
   - c_1 dynamically updated using (2)
   - c_2 and c_3 are randomly generated within [0, 1]
vii) Convergence criterion: Maximum iteration reached or negligible change in duty cycle value
viii) Sampling time: Adjusted according to the simulation step to ensure stable tracking
ix) Simulation environment: ALTAIR PSIM Professional 2022.1.0.8 platform-based dynamic simulation under varying irradiance and temperature conditions

The SSA algorithm continuously updates the SEPIC converter duty cycle to track the maximum power point (MPP). At each iteration, the fitness function is defined as the instantaneous output power of the PV system, which is maximized during the optimization process. This configuration ensures a balance between convergence speed and tracking accuracy, while maintaining stability under dynamic environmental conditions.

2.4. Grey wolf optimization

The GWO is a nature-inspired optimization method derived from the cooperative hunting strategy of grey wolves. The population hierarchy consists of alpha (α), beta (β), delta (δ), and omega (ω) wolves, where the best three candidate solutions guide the movement of the remaining population. The encircling behavior is mathematically represented as (5) and (6).

$$D = \left|C\left(X_p(t) - X(t)\right)\right| \tag{5}$$

$$X(t+1) = X_p(t) - A \times D \tag{6}$$

Where X_p represents the best solution obtained during the searching process. The coefficient vectors are determined using (7) and (8).

$$A = 2a \times r_1 - a \tag{7}$$

$$C = 2r_2 \tag{8}$$

To simulate cooperative hunting, the positions are updated using (9)-(11).

$$D_\alpha = |C_1 X_\alpha - X|;\ D_\beta = |C_2 X_\beta - X|;\ D_\delta = |C_2 X_\delta - X| \tag{9}$$

$$X_1 = X_\alpha - A_1 D_\alpha\ ;\ X_2 = X_\beta - A_2 D_\beta;\ X_3 = X_\delta - A_3 D_\delta \tag{10}$$

$$X(t+1) = \frac{X_1 + X_2 + X_2}{3} \tag{11}$$

The final position updating mechanism combines the influence of the three dominant wolves to direct the population toward the global optimum [26]. In this study, GWO was implemented under identical converter configurations, irradiance profiles, and temperature conditions to establish a balanced comparative evaluation against SSA.

2.5. Modeling SEPIC converter

The SEPIC converter was selected because of its capability to operate in both step-up and step-down modes while maintaining positive output polarity and low output ripple characteristics [27]. In the proposed system, the converter duty cycle is continuously regulated by the MPPT controller to maintain PV operation at the maximum power point. The SSA algorithm dynamically adjusts the duty cycle of the SEPIC converter to maintain operation at the MPP [5].

The (12)-(16) can be used to determine the parameters required for designing a SEPIC converter. The converter topology is illustrated in Figure 3; its design parameters are summarized in Table 1.

$$\mathrm{D} = \frac{\mathrm{Vo}}{\mathrm{Vo+Vs}} \tag{12}$$

$$V_{L1} = V_S = L_1\left(\frac{di_{L1}}{dt}\right) = L_1\left(\frac{\Delta i_{L1}}{\Delta t}\right) = L_1\left(\frac{\Delta i_{L1}}{DT}\right) \tag{13}$$

$$V_{L2} = V_{C1} = V_S = L_2\left(\frac{di_{L2}}{dt}\right) = L_2\left(\frac{\Delta i_{L2}}{\Delta t}\right) = L_2\left(\frac{\Delta i_{L2}}{DT}\right) \tag{14}$$

$$C_1 = \frac{\mathrm{D}}{\mathrm{R}(\Delta V_{C1}/V_O)f} \tag{15}$$

$$C_2 = \frac{\mathrm{D}}{\mathrm{R}(\Delta V_O/V_O)f} \tag{16}$$

Where: V_s is the voltage source (V); V_{L1}, V_{L2} are the voltages across inductor 1 and inductor 2 (V); V_{C1} is the voltage across capacitor 1 (V); V_o is the output voltage (V); D is the duty cycle (%); f is the frequency (Hz); R is the resistor (Ohm); i_{L1}, i_{L2} are currents flowing through inductors $L_1$and L_2(A); Δi_{L1}, Δi_{L2} is inductor current variations during the conduction interval (A); Δt is the time interval over which the current changes (seconds); ΔV_o is the output voltage ripple (V); ΔV_{C1} is the output voltage ripple (V); L_1, L_2 is inductor 1, inductor 2 (Henry); and C_1, C_2 are capacitor 1, capacitor 2 (Farad).

The SEPIC converter parameters used in this study are summarized in Table 1. The switching frequency was fixed at 40 kHz to achieve stable converter operation with low current ripple and fast transient response. To improve practical relevance, converter losses and non-ideal effects were incorporated into the simulation model, including switching losses, conduction losses, and passive component parasitic resistance. Ripple characteristics of the inductor current and output voltage were also analyzed to evaluate converter stability during dynamic irradiance transitions. This approach allows the proposed MPPT system to more accurately represent practical operating conditions prior to future hardware implementation using STM32-based embedded control platforms.

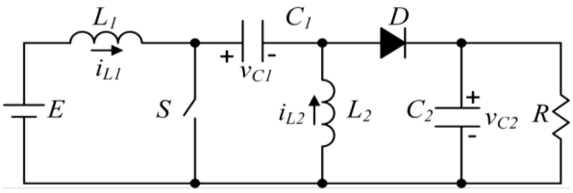

Figure 3. SEPIC converter circuit topology

Table 1. Specification of SEPIC converter

Component	Value
L_1 (Inductor 1)	182.71 μH
L_2 (Inductor 2)	182.71 μH
C_1 (Capacitor 1)	422.2 μF
C_2 (Capacitor 2)	422.2 μF
$C_{snubber}$ (Capacitor snubber)	10 nF
$R_{snubber}$ (Resistor snubber)	330 Ω
Frequency switching	40 kHz

3. RESULTS AND DISCUSSION

The performance evaluation of the SSA and GWO for MPPT was carried out through closed-loop dynamic simulations using the ALTAIR PSIM Professional 2022.1.0.8 platform. The simulation model consisted of a 100 Wp photovoltaic module integrated with a SEPIC converter, voltage and current sensing circuits, battery storage, and embedded control blocks representing the SSA and GWO optimization processes. The complete simulation configuration is illustrated in Figure 4. The analysis focused on the capability of both algorithms to maintain stable operation at the maximum power point under varying irradiance and temperature conditions.

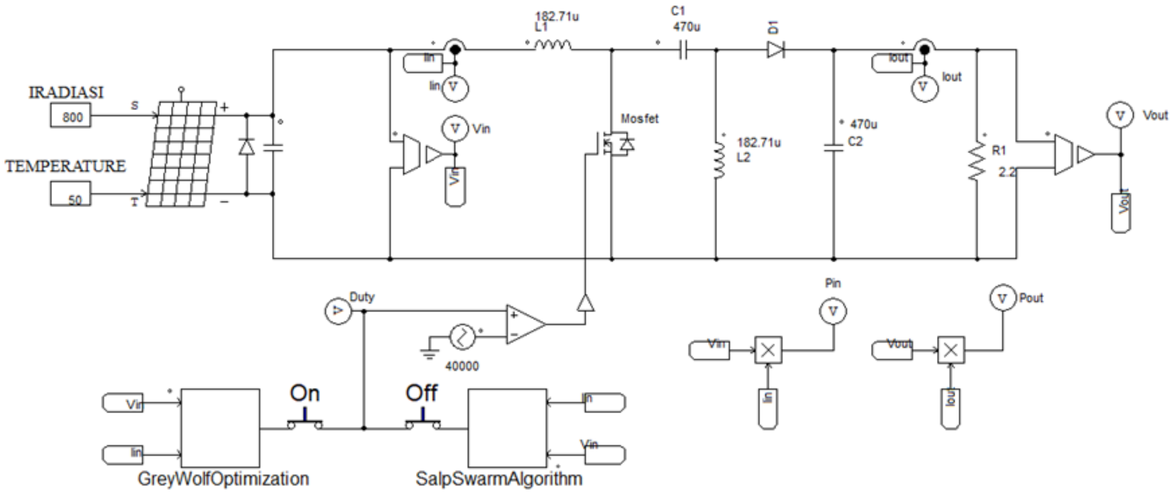

Figure 4. Simulation setup in ALTAIR PSIM Professional 2022.1.0.8 platform

The MPPT controller continuously monitored the PV voltage and current to calculate the instantaneous output power using: $P = V \times I$. The calculated power value was used as the fitness parameter for determining the optimal duty cycle of the SEPIC converter. Under standard test conditions (STC), the photovoltaic module produced a theoretical maximum power of approximately 65.22 W, as presented in Figure 5. This reference value was used to evaluate the tracking performance, convergence behavior, and stability of both optimization techniques.

Figure 6 presents the transient output power response obtained from the SSA-controlled MPPT system. During the initial operating interval, the algorithm entered an exploration stage characterized by moderate oscillatory movement while searching for the optimal operating point. This transient behavior occurred within approximately 0–0.15 s and represents the adaptive searching mechanism of SSA under nonlinear PV characteristics.

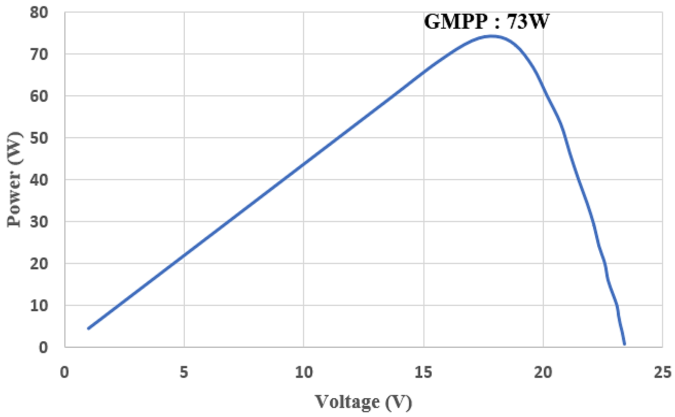

Figure 5. Characteristic curve P-V

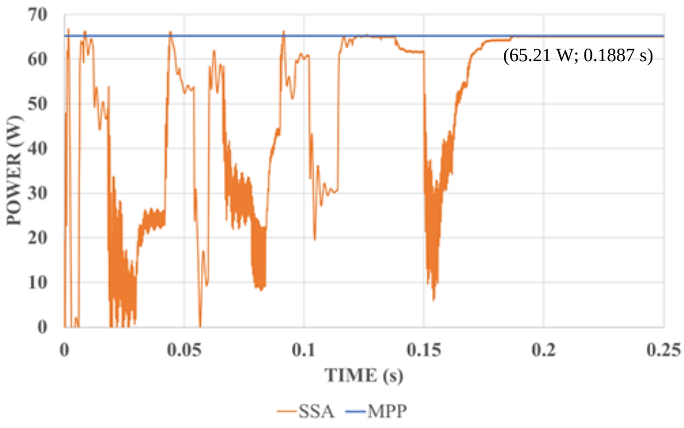

Figure 6. Power output curve of PV system controlled by SSA-based MPPT

After the exploration phase, the output power gradually converged toward the reference maximum power point and stabilized at approximately 65.21 W around 0.1887 s. Once convergence was achieved, the oscillation amplitude decreased significantly, indicating stable steady-state operation and accurate duty cycle regulation of the SEPIC converter. The reduced oscillatory response demonstrates that SSA successfully balances exploration and exploitation processes, enabling rapid convergence without excessive steady-state fluctuation. The simulation results also indicate that SSA maintained stable operation during rapid irradiance transitions. When irradiance levels changed suddenly, the controller was capable of relocating the new maximum power point with minimal overshoot and relatively short recovery time. This behavior confirms the suitability of SSA for dynamic photovoltaic operating environments where irradiance continuously varies due to cloud movement and atmospheric disturbances.

The transient response produced by the GWO-based MPPT system is illustrated in Figure 7. Similar to SSA, the algorithm initially approached the reference maximum power point during the early simulation interval. However, the convergence behavior of GWO exhibited larger oscillation amplitude and less stable steady-state performance.

Although the output power reached approximately 65.16 W near 0.1892 s, the algorithm repeatedly deviated from the optimum operating region during subsequent operation. Several power drops below 20 W were observed, indicating unstable duty cycle adaptation and slower recovery during dynamic irradiance variation. Compared with SSA, the GWO algorithm required a longer stabilization process and produced higher steady-state oscillation around the maximum power point. The instability observed in the GWO response is primarily associated with the position-updating mechanism of the optimization process, which tends to generate wider searching movement under rapidly changing operating conditions. As a result, the converter operates farther from the ideal duty cycle region, causing a temporary reduction in output power and tracking accuracy.

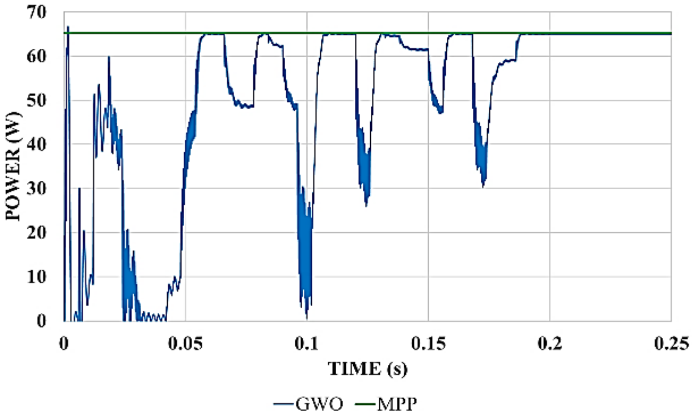

Figure 7. Power output curve of PV system controlled by GWO-based MPPT

Table 2 summarizes the MPPT performance obtained under multiple irradiance and temperature scenarios. The analysis demonstrates that both optimization algorithms were capable of approaching the theoretical maximum power point under high irradiance conditions. Nevertheless, significant performance differences became more apparent as the irradiance level decreased.

At 1000 W/m² and 55 °C, both controllers achieved output power values close to the theoretical MPP. SSA generated 77.53 W, while GWO produced 76.94 W, indicating comparable tracking capability during high-energy operating conditions. Similar behavior was observed at 800 W/m², where both methods successfully maintained output power near the reference MPP value.

Under moderate irradiance conditions of 600 W/m², the superiority of SSA became more noticeable. SSA maintained stable tracking performance with an output power of 51.13 W, whereas GWO experienced significant deviation and only achieved 43.73 W. This difference indicates that SSA possesses stronger adaptability during transient environmental variation. At low irradiance levels of 200 W/m², the performance degradation of GWO became increasingly severe. SSA remained capable of extracting 16.40 W from the available theoretical power of 18.17 W, while GWO only generated 10.49 W. This result demonstrates that SSA provides better robustness and tracking consistency under weak irradiance conditions, where optimization algorithms commonly experience convergence instability.

Table 2. MPPT simulation results under different temperature and irradiance levels

Irradiance (W/m^2)	Temperature (°C)	MPP (W)	Power (W)	
			Salp swarm algorithm	Grey wolf optimization
1000	55	78.11	77.53	76.94
800	50	65.22	65.21	65.16
600	45	51.47	51.13	43.73
400	40	35.58	35.06	35.09
200	35	18.17	16.40	10.49

Figure 8 further compares the dynamic output power responses of SSA and GWO relative to the reference maximum power point. The SSA curve converges more rapidly toward the reference trajectory and maintains smaller steady-state oscillations. Conversely, GWO exhibits wider fluctuations and slower adaptation during transient irradiance changes, leading to reduced tracking precision. A quantitative comparison of tracking efficiency and convergence time is presented in Table 3. The obtained results indicate that SSA consistently achieved higher tracking accuracy across nearly all operating conditions.

Table 3. Results of MPPT simulation accuracy comparison

Irradiance (W/m^2)	Temperature (°C)	Accuracy (%)		MPP time tracking (s)	
		SSA	GWO	SSA	GWO
1000	55	99.25	98.50	0.1790	0.2040
800	50	99.98	99.90	0.1887	0.1892
600	45	99.33	84.96	0.1909	0.1977
400	40	98.53	98.62	0.1952	0.2677
200	35	90.25	57.73	0.3843	0.3147
Average		97.46	87.94	0.2276	0.2346

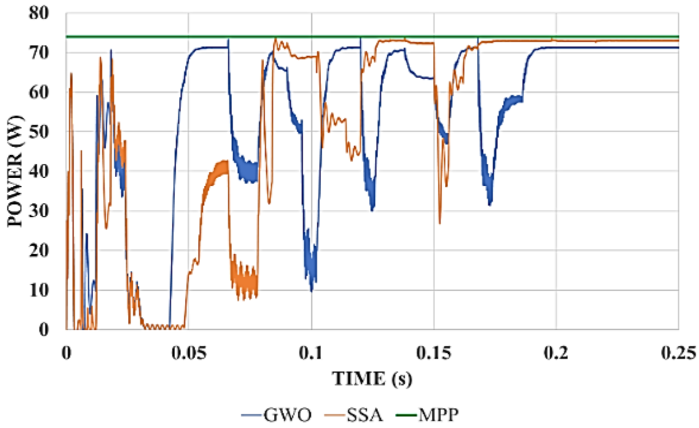

Figure 8. Comparison of output power response between SSA and GWO algorithms

At high irradiance levels, both algorithms produced tracking efficiencies above 98%. However, under medium and low irradiance conditions, the performance gap increased significantly. At 600 W/m², SSA achieved 99.33% tracking accuracy, while GWO decreased to 84.96%. The largest difference occurred at 200 W/m², where SSA maintained 90.25% accuracy and GWO dropped to only 57.73%.

The convergence characteristics also demonstrate the superiority of SSA. The average convergence time achieved by SSA was approximately 0.2276 s, whereas GWO required approximately 0.2512 s. Although the numerical difference appears relatively small, the faster convergence of SSA contributed to reduced transient power loss and improved stability during irradiance variation.

The improved performance of SSA is closely related to its adaptive leader–follower searching mechanism, which enables smoother movement toward the global optimum while preventing excessive oscillation. In contrast, GWO tends to exhibit broader searching trajectories that increase transient instability during rapid environmental changes. In addition to tracking accuracy evaluation, the converter response was analyzed by observing voltage ripple, current ripple, and transient stability during dynamic operating conditions. The SEPIC converter maintained stable operation throughout the simulation period, with acceptable ripple magnitude and fast transient recovery. The inclusion of switching losses, conduction losses, and parasitic resistances in the converter model also demonstrated that SSA remained capable of maintaining stable MPPT operation under non-ideal conditions.

The computational behavior of both algorithms was also evaluated for potential real-time implementation using STM32-based embedded controllers. SSA demonstrated relatively stable convergence with moderate computational complexity, making it suitable for low-power standalone photovoltaic applications requiring rapid tracking response. Although the present investigation was limited to simulation analysis, the obtained results indicate strong potential for future hardware implementation and real-time experimental validation. Overall, the simulation results confirm that SSA provides superior MPPT capability compared with GWO in terms of tracking accuracy, convergence speed, low-irradiance robustness, and dynamic stability. Therefore, SSA can be considered a reliable optimization-based MPPT approach for compact standalone photovoltaic systems operating under continuously changing environmental conditions.

4. CONCLUSION

This study presented a comparative investigation of the SSA and GWO for MPPT in a standalone 100 Wp photovoltaic system employing a SEPIC converter under dynamically changing irradiance and temperature conditions. Based on the simulation results obtained using ALTAIR PSIM Professional 2022.1.0.8 platform, SSA demonstrated superior performance in terms of tracking accuracy, convergence behavior, transient stability, and robustness under low-irradiance operation.

The obtained results indicate that SSA was capable of maintaining output power closer to the theoretical maximum power point across all operating scenarios. The algorithm achieved an average tracking efficiency of 97.46% with an average convergence time of 0.2276 s, whereas GWO produced 87.94% tracking efficiency with a slower convergence response of 0.2512 s. Under low irradiance conditions, SSA remained stable and maintained acceptable tracking performance, while GWO experienced significant oscillation and noticeable power degradation. These findings demonstrate that the adaptive searching mechanism of SSA provides a better balance between exploration and exploitation, enabling faster and more stable duty cycle optimization for MPPT applications.

In addition, the simulation results confirm that SSA is suitable for compact standalone photovoltaic systems requiring rapid response and stable operation under fluctuating environmental conditions. The inclusion of converter non-ideal characteristics, including switching losses, conduction losses, and ripple effects, also indicates that SSA maintains reliable performance under more realistic operating conditions.

Nevertheless, this work remains limited to simulation-based evaluation and does not yet include experimental verification using physical hardware. Factors such as sensor inaccuracy, embedded processing delay, electromagnetic interference, and real-time controller limitations were not comprehensively analyzed in this study. Furthermore, although the proposed investigation compared SSA with GWO, broader benchmarking against conventional MPPT techniques such as P&O, INC, and hybrid optimization approaches is still required for more comprehensive evaluation.

Future research will focus on real-time implementation using embedded platforms such as STM32-based controllers and hardware prototype validation under practical operating conditions. Additional investigations involving partial shading scenarios, computational burden analysis, converter efficiency optimization, and comparative evaluation with other intelligent MPPT methods are also recommended to further examine the scalability and practical applicability of SSA-based MPPT systems in real-world photovoltaic applications.

ACKNOWLEDGMENTS

The authors gratefully acknowledge the support and research facilities provided by Politeknik Elektronika Negeri Surabaya during the completion of this study. This research was conducted as an independent research project and was fully supported through a self-funded research grant provided by the authors. The authors also express their appreciation to all contributors and academic colleagues who provided technical discussions, simulation support, and constructive insights throughout the research process. It is expected that the outcomes of this work will contribute to the advancement of intelligent MPPT control strategies and power electronics applications for photovoltaic energy systems.

FUNDING INFORMATION

This research was carried out through an independent, self-funded research initiative supported by the authors. Additional technical assistance, laboratory facilities, and infrastructural support were provided by Politeknik Elektronika Negeri Surabaya during the completion of this study.

AUTHOR CONTRIBUTIONS STATEMENT

This journal uses the Contributor Roles Taxonomy (CRediT) to recognize individual author contributions, reduce authorship disputes, and facilitate collaboration.

Name of Author	C	M	So	Va	Fo	I	R	D	O	E	Vi	Su	P	Fu
Indhana Sudiharto	✓		✓	✓	✓	✓	✓	✓		✓				✓
Mochammad Machmud Rifadil	✓	✓				✓	✓	✓	✓	✓	✓	✓	✓	✓
Muhammad Affid Febriansyah	✓		✓	✓			✓		✓	✓	✓		✓	

C : **C**onceptualization
M : **M**ethodology
So : **So**ftware
Va : **Va**lidation
Fo : **Fo**rmal analysis
I : **I**nvestigation
R : **R**esources
D : **D**ata Curation
O : Writing - **O**riginal Draft
E : Writing - Review & **E**diting
Vi : **Vi**sualization
Su : **Su**pervision
P : **P**roject administration
Fu : **Fu**nding acquisition

CONFLICT OF INTEREST STATEMENT

The authors affirm that there are no competing interests associated with this study.

DATA AVAILABILITY

All data relevant to this study are provided within the main article and, where applicable, in the accompanying supplementary materials.

REFERENCES

[1] A. F. Mirza, M. Mansoor, Q. Ling, B. Yin, and M. Y. Javed, "A salp-swarm optimization based MPPT technique for harvesting maximum energy from PV systems under partial shading conditions," *Energy Conversion and Management*, vol. 209, p. 112625, Apr. 2020, doi: 10.1016/j.enconman.2020.112625.

[2] S. Mekhilef, R. Saidur, and A. Safari, "A review on solar energy use in industries," *Renewable and Sustainable Energy Reviews*, vol. 15, no. 4, pp. 1777–1790, May 2011, doi: 10.1016/j.rser.2010.12.018.

[3] M. N. I. Jamaludin *et al.*, "An effective salp swarm based MPPT for photovoltaic systems under dynamic and partial shading conditions," *IEEE Access*, vol. 9, pp. 34570–34589, 2021, doi: 10.1109/ACCESS.2021.3060431.

[4] H. Mustapha, *Artificial Intelligence and Renewables Towards an Energy Transition*. Switzerland, 2020.

[5] S. Mirjalili, A. H. Gandomi, S. Z. Mirjalili, S. Saremi, H. Faris, and S. M. Mirjalili, "Salp swarm algorithm: a bio-inspired optimizer for engineering design problems," *Advances in Engineering Software*, vol. 114, pp. 163–191, Dec. 2017, doi: 10.1016/j.advengsoft.2017.07.002.

[6] C. Zeng, B. Yang, P. Cao, Q. Li, J. Deng, and S. Tian, "Current status, challenges, and trends of maximum power point tracking for PV systems," *Frontiers in Energy Research*, vol. 10, Apr. 2022, doi: 10.3389/fenrg.2022.901035.

[7] T. Esram and P. L. Chapman, "Comparison of photovoltaic array maximum power point tracking techniques," *IEEE Transactions on Energy Conversion*, vol. 22, no. 2, pp. 439–449, Jun. 2007, doi: 10.1109/TEC.2006.874230.

[8] M. Yue and X. Wang, "A revised incremental conductance MPPT algorithm for solar PV generation systems," *arXiv preprint arXiv:1405.4890*, 2014, [Online]. Available: https://arxiv.org/abs/1405.4890.

[9] M. A. Ghasemi, H. M. Foroushani, and M. Parniani, "Partial shading detection and smooth maximum power point tracking of PV arrays under PSC," *IEEE Transactions on Power Electronics*, vol. 31, no. 9, pp. 6281–6292, Sep. 2016, doi: 10.1109/TPEL.2015.2504515.

[10] K. Ishaque and Z. Salam, "A review of maximum power point tracking techniques of PV system for uniform insolation and partial shading condition," *Renewable and Sustainable Energy Reviews*, vol. 19, pp. 475–488, Mar. 2013, doi: 10.1016/j.rser.2012.11.032.

[11] A. Safari and S. Mekhilef, "Simulation and hardware implementation of incremental conductance MPPT with direct control method using cuk converter," *IEEE Transactions on Industrial Electronics*, vol. 58, no. 4, pp. 1154–1161, Apr. 2011, doi: 10.1109/TIE.2010.2048834.

[12] A. K. Abdelsalam, A. M. Massoud, S. Ahmed, and P. N. Enjeti, "High-performance adaptive perturb and observe MPPT technique for photovoltaic-based microgrids," *IEEE Transactions on Power Electronics*, vol. 26, no. 4, pp. 1010–1021, Apr. 2011, doi: 10.1109/TPEL.2011.2106221.

[13] L. Vanneschi and S. Silva, "Particle swarm optimization," 2023, pp. 105–111. doi: 10.1007/978-3-031-17922-8_4.

[14] B. Huang *et al.*, "A robust salp swarm algorithm for photovoltaic maximum power point tracking under partial shading conditions," *Mathematics*, vol. 12, no. 24, p. 3971, Dec. 2024, doi: 10.3390/math12243971.

[15] J. Montano, A. F. T. Mejia, A. A. Rosales Muñoz, F. Andrade, O. D. Garzon Rivera, and J. M. Palomeque, "Salp swarm optimization algorithm for estimating the parameters of photovoltaic panels based on the three-diode model," *Electronics*, vol. 10, no. 24, p. 3123, Dec. 2021, doi: 10.3390/electronics10243123.

[16] I. Dagal, B. Akın, and E. Akboy, "Improved salp swarm algorithm based on particle swarm optimization for maximum power point tracking of optimal photovoltaic systems," *International Journal of Energy Research*, vol. 46, no. 7, pp. 8742–8759, Jun. 2022, doi: 10.1002/er.7753.

[17] L. Tightiz, S. Mansouri, F. Zishan, J. Yoo, and N. Shafaghatian, "Maximum power point tracking for photovoltaic systems operating under partially shaded conditions using SALP swarm algorithm," *Energies*, vol. 15, no. 21, p. 8210, Nov. 2022, doi: 10.3390/en15218210.

[18] M. N. I. Jamaludin, M. F. N. Tajuddin, T. Younis, S. B. Thanikanti, and M. Khishe, "Hybrid salp swarm maximum power point tracking algorithm for photovoltaic systems in highly fluctuating environmental conditions," *Scientific Reports*, vol. 15, no. 1, p. 650, Jan. 2025, doi: 10.1038/s41598-024-84333-z.

[19] M. Mao, L. Zhang, L. Yang, B. Chong, H. Huang, and L. Zhou, "MPPT using modified salp swarm algorithm for multiple bidirectional PV-Ćuk converter system under partial shading and module mismatching," *Solar Energy*, vol. 209, pp. 334–349, Oct. 2020, doi: 10.1016/j.solener.2020.08.078.

[20] H. Azli, S. Titri, and C. Larbes, "MPPT - based improved salp swarm algorithm for improving performance and efficiency of photovoltaic system under partial shading condition," 2021, pp. 478–486. doi: 10.1007/978-3-030-63846-7_45.

[21] R. B. A. Koad, A. F. Zobaa, and A. El-Shahat, "A novel MPPT algorithm based on particle swarm optimization for photovoltaic systems," *IEEE Transactions on Sustainable Energy*, vol. 8, no. 2, pp. 468–476, 2017, doi: 10.1109/TSTE.2016.2606421.

[22] M. Castelli, L. Manzoni, L. Mariot, M. S. Nobile, and A. Tangherloni, "Salp swarm optimization: a critical review," *Expert Systems with Applications*, vol. 189, p. 116029, Mar. 2022, doi: 10.1016/j.eswa.2021.116029.

[23] M. Premkumar, C. Kumar, R. Sowmya, and J. Pradeep, "A novel salp swarm assisted hybrid maximum power point tracking algorithm for the solar photovoltaic power generation systems," *Automatika*, vol. 62, no. 1, pp. 1–20, Jan. 2021, doi: 10.1080/00051144.2020.1834062.

[24] C. Mishra and S. Tiwari, "Improved hybrid salp swarm and sine-cosine optimization based MPPT control for PV systems under partial shading conditions," *Journal of Physics: Conference Series*, vol. 2062, no. 1, p. 012022, Nov. 2021, doi: 10.1088/1742-6596/2062/1/012022.

[25] A. Jusoh, O. J. E. Ibrahim Mohammed, and T. Sutikno, "Variable Step Size Perturb and Observe MPPT for PV Solar Applications," *TELKOMNIKA (Telecommunication Computing Electronics and Control)*, vol. 13, no. 1, p. 1, Mar. 2015, doi: 10.12928/telkomnika.v13i1.1180.

[26] A.-A. A. Mohamed, A. A. M. El-Gaafary, Y. S. Mohamed, and A. M. Hemeida, "Multi-objective modified grey wolf optimizer for optimal power flow," in *2016 Eighteenth International Middle East Power Systems Conference (MEPCON)*, Dec. 2016, pp. 982–990, doi: 10.1109/MEPCON.2016.7837016.

[27] A. Elkhateb, N. A. Rahim, J. Selvaraj, and M. N. Uddin, "Fuzzy-logic-controller-based SEPIC converter for maximum power point tracking," *IEEE Transactions on Industry Applications*, vol. 50, no. 4, pp. 2349–2358, Jul. 2014, doi: 10.1109/TIA.2014.2298558.

BIOGRAPHIES OF AUTHORS

Indhana Sudiharto was born in Madiun, Indonesia, in 1966. He received his Bachelor of Engineering degree in power systems from the Sepuluh Nopember Institute of Technology, Indonesia, in 1996, and his Master of Engineering degree in power systems from the same institution in 2006. He is currently an associate professor in the Department of Electrical Engineering at Politeknik Elektronika Negeri Surabaya (PENS), Indonesia. He joined the Division of Industrial Electrical Engineering, Department of Electrical Engineering, Politeknik Elektronika Negeri Surabaya (PENS), as a lecturer in 1996. He heads the Power Quality Research Group at PENS. His research interests include power systems, renewable energy, and power electronics. As a lecturer, he has taught courses such as electrical measurement and instrumentation, electrical power system protection, and power quality. He can be contacted at email: indhana@pens.ac.id.

Mochammad Machmud Rifadil is a lecturer in the Industrial Electrical Engineering Study Program at the Electronic Engineering Polytechnic Institute of Surabaya (EEPIS). He began his academic career by completing a Diploma 4 degree in industrial electrical engineering at PENS and subsequently pursued a master's degree in electrical engineering with a joint curriculum concentration at the Sepuluh Nopember Institute of Technology. His research interests in computer vision include image processing and visual recognition technologies for industrial applications and security systems. In addition, he applies artificial intelligence to develop innovative solutions and has expertise in designing control systems for automation. His areas of specialization support the development of technological solutions that promote energy sustainability and improve efficiency in various industrial systems. With a passion for learning and knowledge sharing, he is committed to producing competent graduates in the field of technology and advancing research in Indonesia. He can be contacted at email: mmrifadil@pens.ac.id.

Muhammad Affid Febriansyah is a student at the Electronic Engineering Polytechnic Institute of Surabaya (EEPIS), Surabaya, Indonesia. He studied in the Industrial Electrical Engineering Department for four years, with coursework covering power electronics, microcontrollers, electrical circuits, computer programming, and intelligent control. He completed a six-month internship at PT Lintech Duta Pratama, Surabaya, in the maintenance section, where he was involved in maintaining and managing the electrical machinery and equipment used in the factory. He can be contacted at email: muhaffid7@gmail.com.